Building and Environment 224 (2022) 109551

Contents lists available at ScienceDirect

Building and Environment

journal homepage: www.elsevier.com/locate/buildenv

Advanced prediction model for individual thermal comfort considering blood glucose and salivary cortisol

Hakpyeong Kim, Dahyun Jung, Heeju Choi, Taehoon Hong *

Department of Architecture and Architectural Engineering, Yonsei University, 50 Yonsei-ro, Seodaemun-gu, Seoul, 03722, Republic of Korea

ARTICLE INFO

Keywords:
Thermal comfort
Bio-signal
Blood glucose
Cortisol
Machine learning

ABSTRACT

Intensified interest in indoor thermal environment has led to an extensive body of research aimed at developing thermal comfort-prediction models with high accuracy. However, previous studies confined the types of bio-signal features due to the limited measuring devices available. Wearable devices for measuring blood glucose (BG) and cortisol (COR) are being developed recently, and the possibility of adding new bio-signal features has been raised. Therefore, this study developed an advanced thermal comfort-prediction model considering BG and salivary cortisol (sCOR) and compared the predictive performance with conventional models. Experiments were conducted to measure the bio-signal features (electrodermal activity, skin temperature, heart rate, blood pressure, BG and sCOR) and psychological measurements of 15 males and 15 females in three conditions: cold, neutral, and warm. To this end, an advanced prediction model was proposed through supervised learning algorithms, including distributed random forest, gradient boosting machine and artificial neural network. The accuracy of the proposed model was 73.4%, yielding 10% better performance than 63.4% of the conventional model. The high feature importance of BG and sCOR demonstrates that these bio-signal features should be included in the prediction model for further studies. The proposed model can be applied in future smart building systems to provide pleasant thermal comfort zones for occupants in general.

1. Introduction

As a result of increased interest in health care and improvement of various sensors, various wearable devices are being developed for bio-signal measurement. In 2021, the global market size for wearable medical devices was recorded at about 21.3 billion USD, and between 2022 and 2030, a compound annual growth rate of 28.1% is expected [1]. Furthermore, increasing awareness of personal health monitoring due to the COVID-19 pandemic has promoted the R&D of wearable devices. As a result, devices not only for sports and fitness, but medical wearable devices that could be used for long-term treatment of patients at home have been developed. For example, people can easily monitor their skin temperature, oxygen saturation, respiratory rate, and heart rate variability by wearing smart wristbands or smart watches from companies like Fitbit, Apple, etc [2,3]. New wearable devices enabled active research on bio-signal measurement and its applications. Among them, research on the relation between bio-signal and thermal comfort is being actively conducted. Interest in thermal comfort is also intensified as an extensive body of research regarding the impact of thermal environment on work productivity and health has been carried out [4–6]. Various bio-signal features were suggested to predict thermal comfort, and the relation between bio-signal and thermal comfort was pointed out. In line with the increasing importance of thermal comfort, a considerable amount of research on the thermal comfort-prediction model has been conducted. Wu et al. improved the general accuracies of classification tree model C5.0, initially about 30% by 15.5% [7]. The bio-signal features used in this study to estimate thermal comfort were skin temperature, blood pressure, and heart rate. Burzo et al. developed an automatic human comfort prediction model using multimodal sensors to collect bio-signal features including heart rate, skin temperature, respiration rate, and electrodermal activity and achieved the highest overall accuracy of 74.4% [8]. Li et al. measured skin temperature using infrared thermography to predict thermal comfort with an average accuracy of 85% [9]. Liu et al. developed an individual thermal comfort-prediction model by collecting bio-signals such as skin temperature and heart rate, and the mean accuracy of their model was 75% [10]. Choi and Yeom proposed the data-driven thermal comfort-prediction model with local body skin temperature and heart rate data collection [11]. As shown in the aforementioned studies, various attempts have been made to increase the predictive accuracy of the thermal comfort-prediction model. But the bio-signal features in

* Corresponding author.
E-mail address: hong7@yonsei.ac.kr (T. Hong).

https://doi.org/10.1016/j.buildenv.2022.109551
Received 15 July 2022; Received in revised form 23 August 2022; Accepted 27 August 2022
Available online 2 September 2022
0360-1323/

Nomenclature

ST	Skin temperature
HRV	Heart rate variability
BP	Blood pressure
HR	Heart rate
EDA	Electrodermal activity
CGMS	Continuous glucose monitoring system
SBGM	Self-blood glucose monitoring
BG	Blood glucose
COR	Cortisol
DRF	Distributed random forest
GBM	Gradient boosting machine
ANN	Artificial neural network
BMI	Body mass index
SBP	Systolic blood pressure
DBP	Diastolic blood pressure
sCOR	Salivary cortisol
PP	Pulse pressure
TSV	Thermal sensation vote
TP[a]	Thermal preference
STAI	State trait anxiety inventory
RRI	Mean RR interval
RMSSD	Root mean square of the successive difference
LF	Lower frequency
HF	High frequency
AUROC	Area of under the receiver operating characteristic curve
AUPRC	Area of under precision-recall curve
TP[b]	True positive
TN	True negative
FP	False positive
FN	False negative
TPR	True positive rate
TNR	True negative rate

most studies that proposed a prediction model were limited to electrodermal activity, skin temperature, blood pressure and heart rate. This is related to the level of the development of wearable device technology that could be applicable to research. In other words, the above bio-signal features can be measured relatively easily by existing wearable devices. As such, it can be surmised that existing studies have focused on developing a thermal comfort-prediction model based on limited bio-signal features.

Recently, a continuous glucose monitoring system has been developed and distributed to substitute for the self-blood glucose monitoring system based on the traditional blood-gathering method. People with diabetes have to monitor their blood glucose at least three to four times daily with a fingerstick, which is the conventional method [12]. On the other hand, continuous glucose monitoring system is a tiny and flat sensor with a needle and can be attached to the skin. The needle in continuous glucose monitoring system measures the blood glucose level by contacting the interstitial fluid in real-time, and when a smartphone makes contact with the sensor, the blood glucose level can be displayed on the screen [13]. At the same time, portable and wearable device that could measure cortisol, also known as the stress hormone, was being developed [14]. Cortisol can be measured using a patch on the skin or contact lens, and further techniques are being developed for market entry [15]. The development of these technologies suggests two points. First, with the help of these technologies, blood glucose and cortisol can be easily measured as the other bio-signal features suggested by previous studies. Thus, adding these two bio-signal features can pave the way for an advanced thermal comfort-prediction model, that is, blood glucose and cortisol are likely to enhance the predictive performance of model. Second, developing wearable and portable devices to measure bio-signal features can contribute to smart building systems. For example, these devices can collect bio-signal features and transfer the data to the cloud to predict occupants' thermal comfort in the near future. It implies that the application of wearable devices to measure blood glucose and cortisol can hold strong practical implications.

A massive number of research play a significant role in clear evidence that thermal comfort is physiologically and psychologically related to stress [16–21]. Thus, it can be inferred that the autonomic nervous system's mechanism impacts thermal comfort. Both blood glucose and cortisol are related to the mechanism of the autonomic nervous system, and there is a possible link between these bio-signal features and thermal comfort [22–25]. However, few studies have dealt with the direct relationship between blood glucose and cortisol and thermal comfort from a short-term perspective. The accuracy of an advanced thermal comfort prediction model that includes blood glucose and cortisol can be improved compared to the conventional models that mainly used electrodermal activity, skin temperature, blood pressure, and heart rate. Therefore, this study aims to propose an advanced thermal comfort-prediction model that considers blood glucose and cortisol and to compare the proposed model to the conventional one. To develop the model, bio-signal features including blood glucose and cortisol of 30 subjects in three different thermal environments were measured. After data collection, some of the features were preprocessed and three supervised learning algorithms namely, distributed random forest, gradient boosting machine, and artificial neural network, were used to develop the prediction model.

2. Materials and methods

2.1. Subjects

This experiment obtained permission from the institutional review board who reviewed the safety and ethics of the experiment, and the approved experiment was conducted based on the specified detailed procedures (IRB no. 7001988-202203-HR-1508-02). Table 1 shows the subjects' demographic statements. A total of 30 subjects participated in the experiment. Since the function of the endocrine system tends to deteriorate by age, the experiment recruited relatively healthy subjects in their 20s and 30s [26]. The age of the female and male subjects was 27.3 ± 3.7 and 29.3 ± 2.4, respectively; the body mass index (BMI) was 20.49 ± 1.87 kg/m^2 and 24.86 ± 2.81 kg/m^2, respectively. None of the subjects were obese or have low body weight based on the BMI classification with a normal weight range of 18.5–24.9 kg/m^2 [27]. Before the recruitment, the research team ran a questionnaire to verify that the

Table 1
Demographic statements.

Criteria	Females (n = 15)	Males (n = 15)
	Mean ± SD	Mean ± SD
Age (year)	27.3 ± 3.7	29.3 ± 2.4
BMI[a] (kg/m^2)	20.5 ± 1.9	24.9 ± 2.8
Fasting retention time (hour)	14.9 ± 2.1	13.1 ± 2.7
Fasting BG[b] level (mg/dL)	90.2 ± 8.5	94.7 ± 8.6
SBP[c] (mmHg)	110.8 ± 8.5	124.8 ± 7.8
DBP[d] (mmHg)	77.3 ± 10.0	80.3 ± 9.2
Average sleep time (hour)	7.4 ± 1.3	7.1 ± 1.1

Note.
[a] *BMI* stands for the body mass index.
[b] *BG* for blood glucose.
[c] SBP for systolic blood pressure.
[d] *DBP* for diastolic blood pressure.

subjects did not have any history of chronic diseases (e.g., diabetes, anemia, hypertension and arrhythmia etc.) related to the autonomic nervous system. In addition, the research team removed external factors that would have a negative effect on the measurement of blood glucose (BG) and cortisol (COR) and set the following exclusion criteria to verify the subjects' normal condition:

- The subjects should not eat anything 8h before the experiment, and their fasting BG level should be between 70 and 100 mg/dL.
- The subjects' systolic blood pressure (SBP) and diastolic blood pressure (DBP) should be below 139 and 89 mmHg, respectively.
- The subjects should have more than 8h of sleep before the experiment, and should refrain from drinking alcohol, smoking or taking drugs 2h before the experiment.

Before the experiment, the research team verified the subjects' BG and BP values and verified the exclusion criteria through the questionnaire. None of the subjects violated the exclusion criteria, and they were all in the normal state, which made it possible for them to participate in the experiment (refer to Table 1).

2.2. Data collection

2.2.1. Environmental factors

This experiment was conducted in an artificial climate chamber (W×D×H: 2.8×3.9×2.4m^3). In the climate chamber, the air temperature can be controlled between 10 and 80°C, and the relative humidity between 10 and 80%. Through the mechanical ventilation system, the air inside can be exchanged with the air outside. Consequently, the experiment could be repeated under an identical thermal environment. Furthermore, the climate chamber was designed to be a typical office space with a desk and chairs. To accurately confirm the air temperature and relative humidity inside the climate chamber, sensors that can comprehensively monitor the indoor air quality surrounding the subjects were installed. The bio-signal data measured by the sensors could be verified in real-time using a computer and a smartphone via the dashboard.

2.2.2. Bio-signals

In this study, the subjects' bio-signal features based on the thermal environment were measured. Aside from the bio-signals that had been measured in related works, this study collected six bio-signal features: (i) electrodermal activity (EDA), (ii) skin temperature (ST), (iii) heart rate (HR), (iv) BP, (v) BG, and (vi) salivary COR (sCOR).

- ***Electrodermal activity (EDA)***: EDA is a bio-signal feature showing the change in skin's electroconductivity due to the sudoriferous action. It is measured by applying a very low voltage on the surface of the skin. This study collected the subjects' EDA data using a wristband (E4 Wristband, Empatica Inc, USA) [28]. EDA generally increases because sweat or other moisture is secreted when humans are under stress due to sympathetic nerve activation. According to Osmalina et al., the EDA can allow for classifying the stress level with over 94% of accuracy [29]. Thus, the EDA can be a biomarker that can be used to define the stress level.
- ***Skin temperature (ST)***: To examine the change in ST based on the thermal environment, this study measured the subjects' ST with the E4 Wristband. ST is regulated by thermoregulation systems with negative and positive feedback to maintain homeostasis [30]. In addition, provoked emotions and induced muscular tension under stress can affect ST.
- ***Heart rate (HR)***: The photoplethysmography sensor inside E4 Wristband measures the blood volume pulse and calculates HR based on the included algorithm [31]. HR refers to heart beats per minute, and it generally tends to increase under stress. The pulse rate tends to increase under stress compared to the state of being at rest [32]. In addition, according to Wu et al., HR tends to drop in a cold environment [33].
- ***Blood pressure (BP)***: BP was measured with an automatic sphygmomanometer (HEM-7600T, Omron, Japan). In particular, SBP, DBP, and Pulse Pressure (PP, difference between SBP and DBP) were measured. When the heart contracts and pushes the blood to the coronary vessels, the BP reaches its maximum, and the BP at this point is called SBP, and when the heart is relaxed, it is called DBP. According to previous studies, BP tends to increase when the human body is under stress [34,35]. In addition, the BP of the body tends to increase further under a cold environment [36].
- ***Blood glucose (BG)***: BG is the concentration of glucose in the blood and is controlled by glucagon, adrenaline and insulin among others. Before the experiment, the subjects' BG level was measured via self-blood glucose monitoring (SBGM), a traditional measurement method for the BG level. SBGM is conducted by taking blood from the tip of a finger using a laser lancing device (LMT-1000, LaMeditech, South Korea) and measuring the BG level with a glucose monitor (Dr. Diary, Dr. Diary Plus, South Korea). A laser lancing device alleviates stress and pain on the subject's part unlike traditional lancing devices. But since the blood collection act itself can cause stress for the subjects, the experiment measured the BG level using a non-invasive method called continuous glucose monitoring system (CGMS). This study used CGMS (FreeStyle Libre 2, Abbott, USA) and collected the BG data with FreeStyle Libre app offered by Abbot.
- ***Salivary cortisol (sCOR)***: COR, a hormone produced by adrenal glands, is shown to be related to the stress level and has often been used as a biomarker for stress [38]. While COR can be collected from blood, urine, saliva or other body fluids, this study used a saliva fluid collection method that could minimize the subjects' stress. In case of sCOR, collection is easy, but its reliability can be poor depending on the mouth's condition. Consequently, this study collected the subjects' saliva using the Salivette kit from Starstedt for accurate sCOR collection [39]. The collected saliva was stored under a refrigerant environment at −20 °C and the refined data were extracted via a professional laboratory.

2.2.3. Psychological measurements

To measure the subjects' thermal comfort and level of anxiety based on the thermal environment, the study conducted surveys based on the three measurements: (i) thermal sensation vote (TSV), (ii) thermal preference (TP), and (iii) state trait anxiety inventory (STAI).

- ***Thermal sensation vote (TSV)***: Thermal sensation is the degree in which the subjects feel the surrounding thermal environment (refer to Table A1). TSV has often been used in tests that analyzed participants' subjective thermal sensation and can evaluate the subjects' thermal sensation on a 7-point Likert scale from −3 (Cold) to +3 (Hot) [40,41].
- ***Thermal preference (TP)***: TP is a subjective criterion on whether subjects prefer the current thermal sensation (refer to Table A2) [42]. This study conducted a survey using a 2-point Likert scale between "1 (Preference)" and "0 (No preference)" to determine the subjects' preference on the thermal environment.
- ***State trait anxiety inventory (STAI)***: STAI consists of state and trait anxiety, which refer to the anxiety that the subject feels temporarily and experiences daily [43]. State anxiety and trait anxiety are measured using 20 questions each where each question is evaluated using four criteria divided by frequency and degree (refer to Table A3 and A4). This study allocated 1 to 4 points to each criterion and summed all points to analyze state anxiety and trait anxiety, respectively. It then analyzed how much the subjects felt anxious under the measurement of state anxiety compared to the normal state by determining the difference between state anxiety and trait anxiety. This study offered questionnaires translated into Korean so that the subjects do not mistranslate each question on the STAI.

2.3. Experimental procedure

Before the experiment, the subjects were given a detailed explanation about the equipment they would wear and the experimental procedures. Next, the research team verified whether the subjects corresponded to the set exclusion criteria and acquired the subjects' agreement to the experiment by receiving their signature on the form. Attached on one arm of the subjects was the CGMS for the measurement of BG and on the other arm was the automatic sphygmomanometer and E4 wristband. After the attachment of CGMS, the subjects waited for about 1 h until compensation of BG value is completed. At the same time, the subjects completed STAI-X-2, which evaluated their trait anxiety. Fig. 1 shows the experimental procedure. The experiment lasted for a total of 80 min, including three phases that took 20 min each. After completion of each phase, the subjects rested for 10 min outside the climate chamber. Since there is no standard for determining appropriate test time, exposure and rest time were determined by referring to previous research with a similar experimental procedure. The thermal environment in Phase 1, 2 and 3 was set at 0, -3, and +3, respectively, according to the predicted mean vote (PMV). Specifically, Phase 1 was set to the neutral condition where PMV was 0 (i.e., 25 °C for temperature and 50% for humidity), Phase 2 was set as the cold condition where PMV was −3 (i.e., 16 °C for temperature and 30% for humidity), and Phase 3 was the warm condition where PMV was +3 (i.e., 33 °C for temperature and 80% for humidity). When the experiment began, the research team monitored EDA, ST, and HR by running the E4 wristband on the subjects. On the other hand, BG, BP and sCOR measurement was done directly by the research team. 5, 10, and 15 min after the beginning of the experiment, the research team measured BG and BP, and after 10 min, sCOR was measured additionally. At the same time, the subjects responded to the survey on TSV and TP after 5, 10, and 15 min of the experiment, and responded to STAI-X-1 upon completion of each phase.

2.4. Machine learning based thermal comfort-prediction model

As shown in Fig. 2, the collected raw bio-signal features were used in data preparation, training, and evaluation in sequence to develop a thermal comfort-prediction model. Ultimately, the study evaluated and compared the prediction performance of the conventional model and the proposed model. The two prediction models were both defined as a binary classification model with TP as its target variable. The prediction variables of the conventional model consisted of the indexes related to EDA, ST, HR and BP, while those of the proposed model consisted of the indexes related to EDA, ST, HR, BP, BG and sCOR.

2.4.1. Data preparation

The raw bio-signal features were refined so that they become suitable for training the machine learning algorithm. Toward this end, the study performed signal processing on the continuous measurement values of EDA and HR. Using Ledalab, MATLAB-based signal analysis software, the study preprocessed and analyzed the raw EDA signal [44]. After the preprocessing including down-sampling, low-pass filtering and smoothing, the signal was decomposed into tonic and phasic components via continuous decomposition analysis. Since the experiment aims to measure the continuous and long-term bio-signal features that change depending on the thermal environment, the study extracted the tonic components. Kubios heart rate variability (HRV) software was also used to preprocess and analyze the raw HR signal [45]. Previous studies show that the HR signal is generally converted into HRV and used as various application indexes. HRV is divided into the time domain indicator based on the time interval between nearby QRS complexes and the frequency domain indicator based on the signal's waveform. This study used the following HRV related indicators as predicator variables based on versatility: (i) Mean HR, (ii) Mean RR interval (RRI), (iii) Root mean square of the successive differences (RMSSD), and (iv) Ratio of lower frequency (LF) (0.04–0.15 Hz) to high frequency (HF) (0.15–0.4 Hz) or just LF/HF ratio.

Next, the study processed the outliers included in the bio-signal feature dataset. The dataset with outliers can result in a distorted or biased performance of the prediction model. An outlier was defined as the value exceeding the dataset's 1.5 x interquartile range (IQR), which substituted for the mean value. Additionally, the study performed a log transformation to convert the biased distribution of the bio-signal feature dataset that showed severe variation among individuals to a normal distribution. Furthermore, the study unified the scale among the predicator variables through min-max normalization by converting the dataset into values between 0 and 1. In summary, there were nine predicator variables of the conventional model: 'EDA', 'ST', 'mean HR', 'mean RRI', 'RMSSD', 'LF/HF ratio', 'SBP', 'DBP' and 'PP', and the target variable was set to 'TP'. On the other hand, the proposed model added to the existing nine predictor variables 'BG' and 'sCOR', and the target variable was identical to 'TP'.

2.4.2. Machine learning algorithm

This study used three supervised learning algorithms to produce the thermal comfort-prediction model: (i) distributed random forest (DRF), (ii) gradient boosting machine (GBM), and (iii) artificial neural network (ANN). According to Joseph [46], optimal train and test data splitting ratio is $\sqrt{p}$: 1, where p is the number of parameters. The number of parameters in DRF, GBM and ANN is 10, 11 and 10, individually. Therefore, 70% of the collected bio-signal feature dataset was allocated to the training set, and 30% to the test set. Next, via the 5-cross validation, the hyperparameters of the supervised learning algorithm were determined, and the study performed a grid search via several iteration processes to extract the optimal predictive performance. For DRF, hyperparameters including 'number of trees' and 'maximum depth' were determined from the grid search. For GBM, hyperparameters such as 'number of trees', 'maximum depth', 'sample rate', 'minimum rows' were determined from the grid search. For ANN, hyperparameters including 'number of hidden layers', 'number of neurons', 'learning

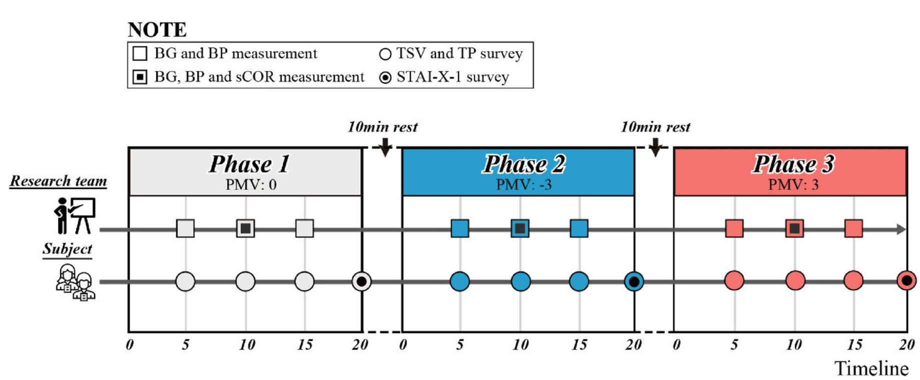

Fig. 1. Experimental procedure.

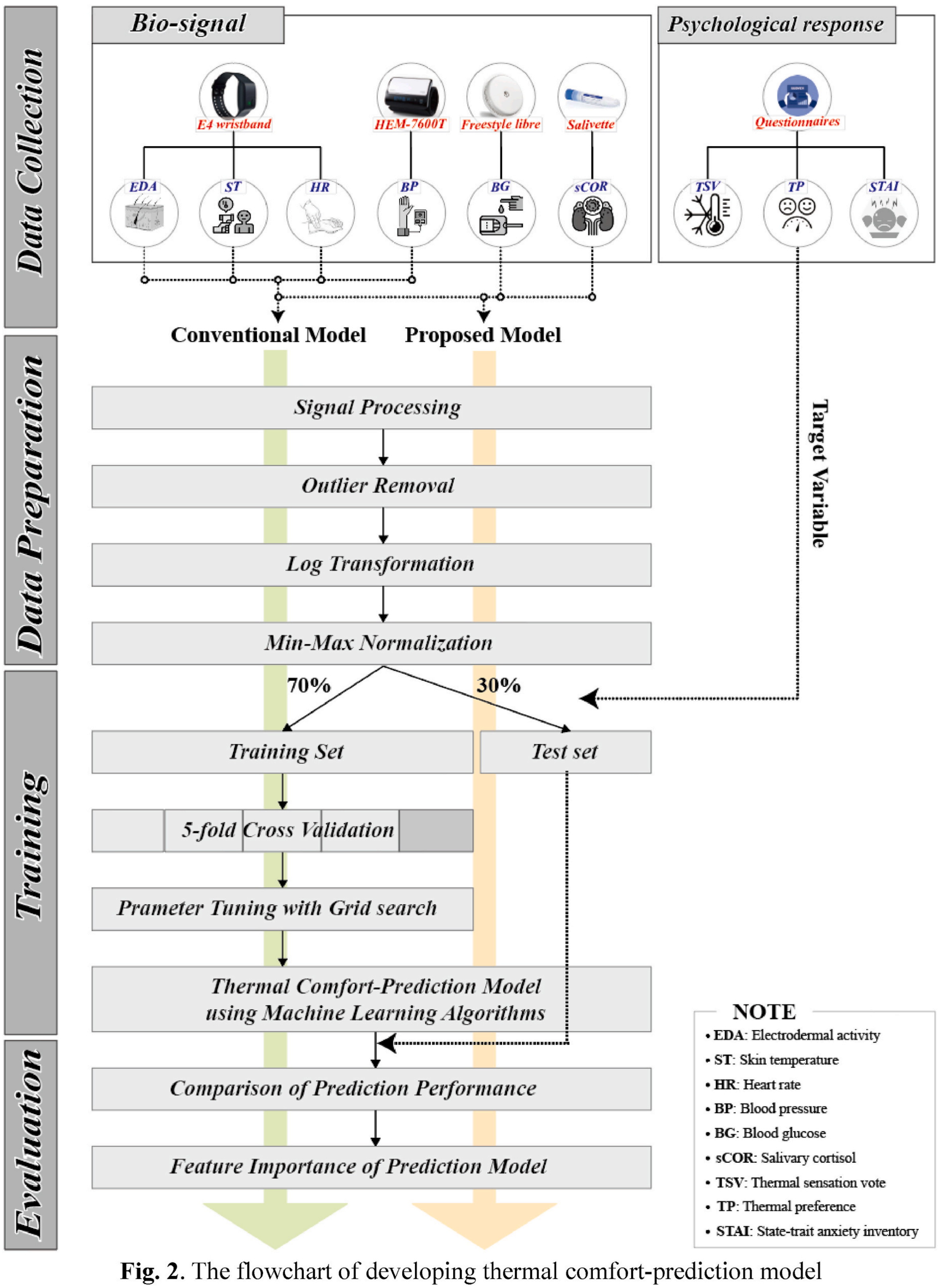

Fig. 2. The flowchart of developing thermal comfort-prediction model.

rates', and 'epoch' were determined from the grid search.

2.4.3. Performance assessment

In the machine learning algorithms where the hyperparameters are set by 5-cross validation, the test set evaluates the predictive performance. The predictive performance was evaluated based on Accuracy, Area under the receiver operating characteristic curve (AUROC) and Area under the precision-recall curve (AUPRC). The aforementioned indexes are produced by the following four parameters that originated from the confusion matrix: (i) true positive (TP), (ii) true negative (TN),

(iii) false positive (FP), and (iv) false negative (FN). TP refers to the number of cases correctly identified as thermal comfort; FP is the number of cases incorrectly identified as thermal comfort; TN is the number of cases correctly identified as thermal discomfort; FN is the number of cases incorrectly identified as thermal discomfort. The ROC curve signifies the relation between the true positive rate (TPR) or recall and the true negative rate (TNR), while the area below the curve is defined as AUROC. The precision-recall curve signifies the relation between TPR or recall and precision and the area below the curve is defined as AUPRC. TPR, TNR, precision, and accuracy can be expressed in Eqs. (1)–(4), respectively. AUROC and AUPRC are often used to evaluate the predictive performance of the dataset with class imbalance. Realistically, the rate in which the target variable TP is 0 (No preference) is higher than 1 (Preference), the study selected AUROC and AUPRC as the indicators for evaluating the predictive performance due to the characteristic of the model, that is, it should more accurately predict the resident's thermal discomfort.

$$TPR\ or\ Recall = \frac{TP}{TP + FN} \times 100\% \tag{1}$$

$$TNR = \frac{TN}{TN + FP} \times 100\% \tag{2}$$

$$Precision = \frac{TP}{TP + FP} \times 100\% \tag{3}$$

$$Accuracy = \frac{TP + TN}{TP + TN + FP + FN} \times 100\% \tag{4}$$

where, TPR stands for true positive rate; TP for true positive; FN for false negative; TNR for true negative rate; TN for true negative; and FP for false positive.

Finally, the study calculated the feature performance to analyze which bio-signal features among the 11 predictor variables showed the highest predictive performance. DRF, GBM and ANN algorithms are all black box models, so it is difficult to determine the importance using a statistical method. Consequently, the study defined the feature importance by conducting data permutation based on random shuffling.

3. Results

3.1. Exploratory data analysis

3.1.1. Outcomes of thermal environment

Table 2 shows the mean value and standard deviation of initial designed and measured environmental condition by the monitoring sensor. For phases 1 and 2, PMV is −0.14 and −2.94, respectively, which is close to the PMV value set initially. For phase 3, PMV is 2.69, which initially has an error of 0.31 from PMV set. In other words, the subjects participated in the experiment in a relatively hot environment in Phase 3. This is because, as the subjects stay in the climate chamber for a long time, the CO_2 concentration increased, which made the mechanical ventilation system run to supply outdoor air to the chamber.

Fig. 3(A) shows the stacked bar chart of the subjects' response for TSV. For phase 1, 66.7% of subjects perceived the thermal environment as neutral condition; 20% of subjects felt warm; 13.3% of subjects felt cool. For phase 2, 87.2% of subjects perceived the thermal environment as cool condition; 12.8% of subjects felt neutral. For phase 3, 92.1% of subjects perceived the thermal environment as warm condition. Fig. 3 (B) shows bar chart of the subjects' response for TP. For phase 1, 84.5% of the subjects responded that the thermal environment was 'Preference'. Conversely, for phases 2 and 3, 65.4 and 76.2% of subjects responded that the thermal environment was 'No preference'.

Table 3 shows the subjects' response for STAI. Trait anxiety was 37.6 ± 7.9, so most subjects were shown to have naturally low emotional anxiety. For the quantitative evaluation of stress caused by the thermal environment, the study should verify the score where the trait anxiety was removed from the state anxiety. The study evaluated the subjects' stress in each phase by calculating the rate of change (%) between the trait anxiety and the state anxiety. For phase 1, the rate of change was −4.95%, showing that the subjects did not feel anxiety and felt calmer than normal. On the other hand, the rate of change in Phase 2 and Phase 3 was 1% and 4.85%, respectively, showing that the subjects felt more anxious than normal. In particular, since the rate of change in phase 3 was higher than in phase 2, it showed that the subjects felt more anxious when it is warm compared to when it is cold.

3.1.2. Outcomes of bio-signal features

The box plot of the collected data is shown in Fig. 4. The EDA of the subjects by thermal environment in Phase 1, 2 and 3 was 0.35 ± 0.19, 0.40 ± 0.21 and 0.44 ± 0.17 μS, respectively. As the value based on the level of sweat secretion, EDA has a relatively high variation among individuals, resulting in high standard deviation. When verified with the mean value, EDA posted a marked increase in Phase 3 than in Phase 1, which was attributed to sweat secretion caused by temperature increase and stress. By phase, ST was 32.2 ± 1.3, 31.3 ± 1.3 and 31.5 ± 2.0 °C, respectively. It showed the highest value in Phase 1, and in Phase 2 and Phase 3, it fell by a bit. HR in Phase 1, 2 and 3 was 72.3 ± 4.6, 65.7 ± 6.4 and 73.9 ± 8.0 beats/min, respectively, showing that the value tended to drop as the subjects felt cold. In particular, when compared to Phase 1, it was more marked in Phase 2, which was a cold environment, than in Phase 3, which was a warm environment. BP is divided into SBP and DBP, and in Phase 1, they were 112.8 ± 9.0 and 76.6 ± 9.0 mmHg, respectively. In addition, in Phase 2 they were 119.3 ± 11.8 and 82.6 ± 9.6 mmHg, respectively. Finally in Phase 3, they were 113.1 ± 9.7 and 75.8 ± 7.8 mmHg, respectively. Generally, BP tended to drop when the subjects felt warm, and the difference was more marked in cold environment than in warm condition compared to the neutral condition. BG was measured to be 77.3 ± 13.3, 71.1 ± 12.1 and 65.0 ± 14.0 mg/dL per phase. Such a result is intensified through the drop in the thermal comfort leading to the drop in BG. sCOR in Phase 1, 2 and 3 was 0.1 ± 0.04, 0.14 ± 0.1 and 0.11 ± 0.06 μg/ml, respectively. Compared to sCOR in Phase 1 was measured to be higher, regardless of temperature, which shows that the drop in thermal comfort increased sCOR.

3.2. Performance assessment of thermal comfort-prediction model

The study evaluated the predictive performances (i.e., accuracy, AUROC and AUPRC) of the thermal comfort-prediction model developed by three machine learning algorithms (i.e., DRF, GBM and ANN). First, compared to the conventional model, the study evaluated the performance of the proposed model that included BG and sCOR. Additionally, the collected bio-signal feature dataset was divided by (i) gender and (ii) thermal state and were used to evaluate the predictive performance of each model.

Table 2
Mean value and standard deviation of designed and measured conditions.

Designed conditions	Measured conditions			
PMV[a]	PMV	Temperature (°C)	Humidity (%)	CO_2 (ppm)
0 (Phase 1)	−0.14	25.4 ± 0.1	36.3 ± 8.3	655.6 ± 161.2
−3 (Phase 2)	−2.94	15.9 ± 2.0	41.6 ± 5.7	821.1 ± 204.8
3 (Phase 3)	2.69	32.7 ± 2.0	59.5 ± 19.5	926.1 ± 233.8

Note.
[a] *PMV* stands for predicted mean vote.

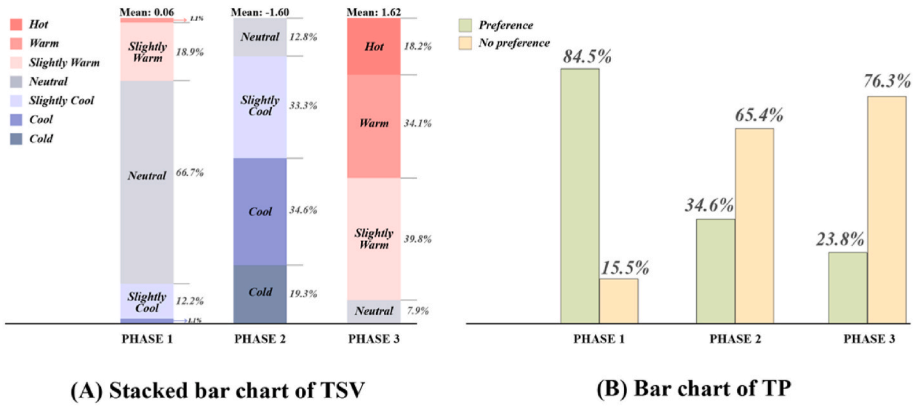

Fig. 3. Bar chart of the subjects' response for TSV and TP.

Table 3
Mean value and standard deviation of subjects' response for STAI.

Phase	Trait anxiety	State anxiety	Rate of change (%)
Phase 1	37.6 ± 7.9	35.0 ± 7.5	−4.95
Phase 2		37.8 ± 8.6	1
Phase 3		38.1 ± 6.7	4.85

3.2.1. *Assessment of proposed model compared to conventional model*

Table 4 shows the predictive performance of one conventional model and three proposed models. Performance assessment was performed after segregation following four cases: (i) conventional model including nine variables (C), (ii) proposed model with BG (C + BG), (iii) proposed model with sCOR (C + sCOR), and (iv) proposed model with BG and sCOR (C + BG + sCOR). For the conventional model, GBM was the algorithm that showed the highest predictive performances (accuracy: 63.4%, AUROC: 67.5%, AUPRC: 66.7%). For 'C + BG', the accuracy of ANN and AUROC was shown to be superior at 69.6 and 71.9%, respectively, and AUPRC of GBM was shown to be highest at 69.5%. For 'C + sCOR', ANN showed the highest predictive performances (accuracy: 69.6%, AUROC: 76.7%, AUPRC: 75.5%). For 'C + BG + sCOR', ANN showed the highest predictive performances (accuracy: 73.4%, AUROC: 77.5%, AUPRC: 78.2%).

Compared to the conventional model, the accuracy, AUROC and AUPRC increased on the average by 3.3, 5.3 and 4%, respectively when BG was added, by 4.3, 8.0 and 8.2% on the average when sCOR was added, and by 9.5, 10.9 and 11.2% on the average when both BG and sCOR were added. sCOR increased the predictive performance of the prediction model more than BG did, and when the two new bio-signal features were all added to the prediction model, its predictive performance increased at its highest.

Fig. 5 shows feature importance of proposed model including BG and

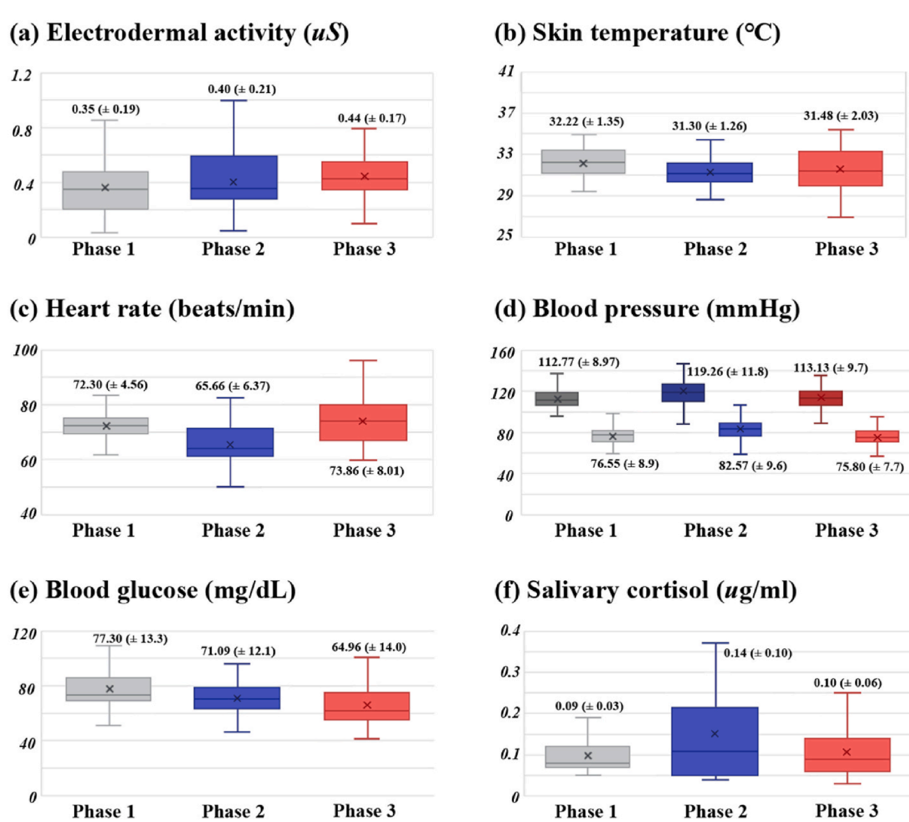

Fig. 4. Box plot of six bio-signal features.

Table 4
Comparison of predictive performance between conventional and proposed models.

Algorithms	Performance	Conventional model (9 variables)	Proposed Models		
			C[g] + BG[h] (10 variables)	C + sCOR[i] (10 variables)	C + BG + sCOR (11 variables)
DRF[a]	ACC[d] (%)	56.1	59.9	60.8	67.0
	AUROC[e] (%)	57.3	64.2	65.4	70.1
	AUPRC[f] (%)	56.6	58.5	65.9	67.1
GBM[b]	ACC (%)	63.4	63.5	65.9	68.4
	AUROC (%)	67.5	68.0	69.4	72.6
	AUPRC (%)	66.7	69.5	67.6	72.9
ANN[c]	ACC (%)	60.8	69.6	69.6	73.4
	AUROC (%)	62.8	71.3	76.7	77.5
	AUPRC (%)	61.2	68.4	75.5	78.2
AVRAGE	ACC (%)	60.1	64.3	65.4	69.6
	AUROC (%)	62.5	67.8	70.5	73.4
	AUPRC (%)	61.5	65.5	69.7	72.7

Note.
[a] *DRF* stands for the distributed random forest.
[b] *GBM* for the gradient boosting machine.
[c] *ANN* for the artificial neural network.
[d] *ACC* for accuracy.
[e] AUROC for area of under the receiver operating characteristic curve.
[f] AUPRC for area of under the precision-recall curve.
[g] *C* for the conventional model.
[h] *BG* for blood glucose.
[i] *sCOR* for salivary cortisol.

sCOR. In sum, RMSSD's feature importance was highest at 12.4%, followed by BG and sCOR at 11.8 and 10.5%, respectively. RMSSD indicates the activity of the parasympathetic nerve to the heart. In other words, this index related to stress level of autonomous nerve system. Such results demonstrate that compared to other bio-signal features that were often used in existing studies, BG and sCOR play a more significant impact on the predictive performance of the thermal comfort-prediction model.

3.2.2. *Assessment in the gender perspective*

The hypothesis that the thermal comfort zone is set differently by gender characteristic is supported by a considerable number of literature and is being proved by active research [47–51]. To examine the gender difference in the psychological and physiological response, the study classified 15 females and 15 males into two groups and developed a thermal comfort-prediction model and evaluated its predictive performance. Moreover, when BG and sCOR were added to the predictive variables of the prediction model, the study identified the changes in the predictive performance of the model.

The bio-signal dataset of the female group was 135 in total, where 71 responded that TP was "1 (Preference)" while 64 responded it to be "0 (No preference)". As shown in Table 5, the study compared the predictive performance of the conventional and proposed models for the female group. For the conventional model, ANN was shown to be the algorithm with the highest predictive performances (accuracy: 77.0%, AUROC: 76.7%, AUPRC: 75.5%). For the proposed model, similarly, ANN was shown to offer the highest predictive performances (accuracy: 69.2%, AUROC: 72.4%, AUPRC: 80.5%). However, when BG and sCOR were aided to the prediction model for the female group, the average predictive performance was rather shown to have dropped. As a result, compared to the conventional model, the proposed model showed a drop in accuracy and AUROC by about 12.4 and 2.9%, respectively. On the other hand, AUPRC increased by about 13.5%, showing that precision changed more sensitively than recall.

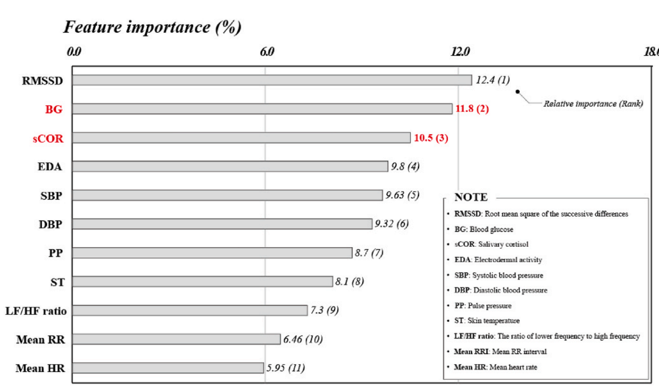

Fig. 5. Feature importance of prediction model considering BG and sCOR.

The bio-signal dataset of the male group was 123 in total, where 55 responded that TP was "1 (Preference)" while 68 responded it to be "0 (No preference)". As shown in Table 5, the study compared the conventional and proposed models' predictive performance for the male group. For the conventional model, ANN was shown to be the algorithm with the highest predictive performances (accuracy: 80.4%, AUROC: 84.8%, AUPRC: 85.7%). For the proposed model, similarly, ANN was shown to offer the highest predictive performances (accuracy: 86.2%, AUROC: 88.5%, AUPRC: 90.0%). Generally, the prediction model of the male group was much superior to that of the female group. Additionally, when BG and sCOR were added to the prediction model of the male group, the predictive performance soared. As a result, compared to the conventional model, the proposed model's accuracy, AUROC and AUPRC increased by about 7.0, 4.7 and 6.0%, respectively.

Fig. 6 shows feature importance of the prediction model in each gender group. Since the prediction model of the two gender groups showed the highest performance with ANN, the study calculated feature importance based on the data permutation using random shuffling. The analysis showed that sCOR was the most significant bio-signal feature in both gender groups. Particularly, in the female group, the feature importance of sCOR was 19.2%, twice higher than the other features. Furthermore, BG was the third most important feature in the female group, and the second more important feature in the male group. As a result, both sCOR and BG were relatively more important in the two gender groups than other bio-signal features.

Gender difference in thermal comfort zone has been actively researched, and various research outcomes have been produced. Indraganti et al. reported that females felt non-neutral sensations and thermal discomfort more than males do [52]. Liu et al. investigated that females were more sensitive to the surrounding thermal environment

Table 5
Comparison of predictive performance in perspective to gender differences.

Algorithms	Performance	Females (n = 15)		Males (n = 15)	
		Conventional model (9 variables)	Proposed Model (11 variables)	Conventional model (9 variables)	Proposed Model (11 variables)
DRF[a]	ACC[d] (%)	63.6	50.0	73.1	83.3
	AUROC[e] (%)	59.3	57.6	76.3	82.2
	AUPRC[f] (%)	53.3	71.0	75.6	82.5
GBM[b]	ACC (%)	71.6	55.8	78.0	83.0
	AUROC (%)	67.7	63.7	83.6	88.2
	AUPRC (%)	61.6	76.6	82.8	89.6
ANN[c]	ACC (%)	77.0	69.2	80.4	86.2
	AUROC (%)	75.4	72.4	84.8	88.5
	AUPRC (%)	72.6	80.5	85.7	90.0
AVRAGE	ACC (%)	70.7	58.3	77.2	84.2
	AUROC (%)	67.5	64.6	81.6	86.3
	AUPRC (%)	62.5	76.0	81.4	87.4

Note.
[a] *DRF* stands for the distributed random forest.
[b] *GBM* for the gradient boosting machine.
[c] *ANN* for the artificial neural network.
[d] *ACC* for accuracy.
[e] AUROC for area of under the receiver operating characteristic curve.
[f] AUPRC for area of under the precision-recall curve.

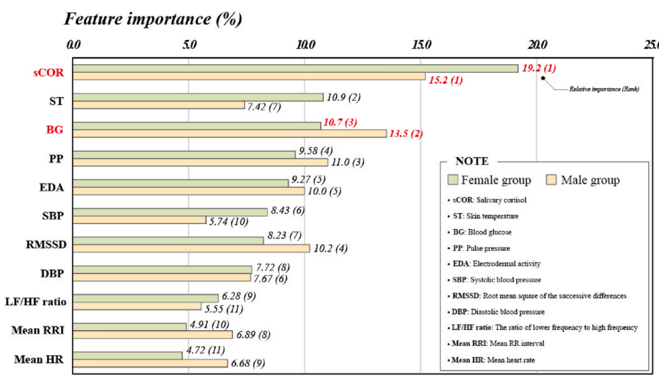

Fig. 6. Feature importance of prediction model in each gender group.

than males due to the skin temperature of particular parts [53]. Xiong et al. concluded that male occupants have stronger thermoregulation ability than female occupants [54]. The results from the aforementioned literature stress that the thermal comfort zone differs by male and female subjects, and that there also is difference in the innate thermoregulation ability. Thus, it is necessary to consider gender characteristics when developing a thermal comfort-prediction model in the future. Choi and Yeom developed a prediction model by identifying gender as the predictor variable, verifying that the predictive accuracy increased from 83.37% to 88.52% [55]. Likewise, Chaudhuri et al. considered gender and confirmed that the predictive accuracy increased from 82.32% to 97.15% [56]. This result showed that gender characteristics significantly influenced the prediction model's performance among the human factors. Furthermore, there is clear scientific evidence that the variation of BG and the amount of COR secretion are affected by gender difference [57–59], and the proposed thermal comfort-prediction model showed a completely opposite result in sCOR and BG between the two-gender group. In summary, if all bio-signal features and thermal comfort zone by gender are considered, the prediction model could produce higher predictive accuracy in the future.

3.2.3. Assessment in the thermal state perspective

The thermal comfort and satisfaction felt by occupants yield different trends by the indoor thermal state (i.e., neutral, cold and warm condition). Many researchers have attempted to verify such a hypothesis by conducting various experiments. Various research outcomes resulted, showing that thermal comfort zones differ according to the weather and climate conditions where people live in. Toward this end, the study divided the dataset collected in Phases 1 and 2 and the dataset collected in Phases 1 and 3 by cold and hot condition, respectively, to develop a thermal comfort-prediction model and evaluated its predictive performance. Moreover, the study confirmed the changes in the predictive performance of the prediction model when BG and sCOR were added to its predictor variables.

The bio-signal dataset in cold condition were 165 in total, and those responding to TP as "1 (Preference)" were 103, and those to "0 (No preference)" were 65. As shown in Table 6, the study compared the conventional and proposed models' predictive performance in cold conditions. For the conventional model, ANN was shown to have the highest predictive performances (accuracy: 70.1%, AUROC: 77.4%, AUPRC: 85.6%). For the proposed model, similarly, ANN was the algorithm with the highest predictive performances (accuracy: 83.0%, AUROC: 83.3%, AUPRC: 83.5%). When BG and sCOR were added to the prediction model in cold conditions, its predictive performance increased. As a result, compared to the conventional model, the proposed model showed an increase in accuracy, AUROC and AUPRC by about 7.5, 4.9 and 0.9%, respectively.

The bio-signal dataset in warm condition were 180 in total, and those responding to TP as "1 (Preference)" were 99, and those to "0 (No preference)" were 81. As shown in Table 6, the study compared the conventional and proposed models' predictive performance in cold conditions. For the conventional model, DRF was shown to have the highest predictive performances (accuracy: 74.1%, AUROC: 78.3%, AUPRC: 71.8%). For the proposed model, similarly, DRF was the algorithm with the highest predictive performances (accuracy: 86.2%, AUROC: 88.5%, AUPRC: 90.0%). Additionally, when BG and sCOR were added to the prediction model in warm condition, its predictive performance was shown to increase significantly. As a result, compared to the conventional model, the proposed model showed an increase in accuracy, AUROC and AUPRC by about 12.4, 8.1 and 12.4% respectively. Generally, the prediction model in warm condition was shown to have slightly better predictive performance than in cold condition, and the degree of the increase in the predictive performance when BG and sCOR were added to the predictor variables was higher in warm condition.

Fig. 7 shows the feature importance (%) of prediction model in two thermal states. In cold condition, it was determined by data permutation using random shuffling, and in warm condition, it was by the mean decrease of Gini index. In the cold condition, BG (11.3%) was shown to

Table 6
Comparison of predictive performance in perspective to thermal state

Algorithms	Performance	Cold condition (PMV=-2.98)		Warm condition (PMV=2.76)	
		Conventional model (9 variables)	Proposed Model (11 variables)	Conventional model (9 variables)	Proposed Model (11 variables)
DRF[a]	ACC[d] (%)	53.4	57.7	65.0	73.1
	AUROC (%)	68.9	75.6	71.9	77.9
	AUPRC (%)	79.0	81.8	65.0	72.7
GBM[b]	ACC (%)	52.8	58.3	74.1	80.0
	AUROC (%)	71.7	73.9	78.3	80.7
	AUPRC (%)	81.4	80.5	71.8	73.0
ANN[c]	ACC (%)	70.1	83.0	64.2	76.6
	AUROC (%)	77.4	83.3	68.5	84.3
	AUPRC (%)	85.6	86.5	56.7	85.0
AVRAGE	ACC (%)	58.8	66.3	67.8	76.6
	AUROC (%)	72.7	77.6	72.9	81.0
	AUPRC (%)	82.0	82.9	64.5	76.9

Note: *DRF*[a] stands for the distributed random forest; *GBM*[b] for the gradient boosting machine; *ANN*[c] for the artificial neural network; *ACC*[d] for accuracy; AUROC[e] for area of under the receiver operating characteristic curve; and AUPRC[f] for area of under the precision-recall curve.

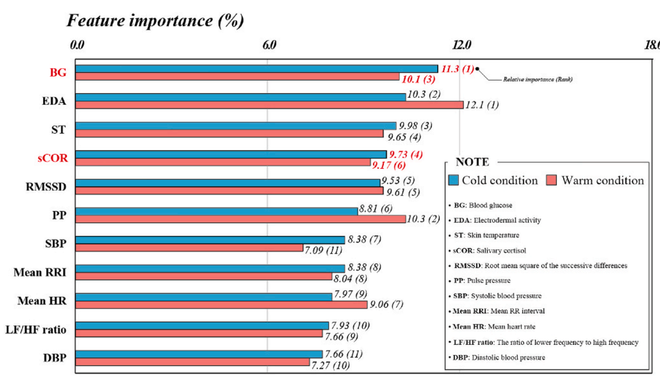

Fig. 7. Feature importance of prediction model in two thermal states.

be the most important bio-signal feature, sCOR (9.73%) was the fourth most. When it is warm, BG (10.1%) was the third, and sCOR (9.17%) was the sixth most important feature.

Previous literature has analyzed the trends in occupants' bio-signal by thermal state. Xiong et al. investigated that thermal state has strong impact on human's bio-signal (i.e., ST) and psychological response (i.e., thermal acceptance) [60]. Hu et al. reported that the change in physiological response (i.e., ST, HR, oxygen saturation and dopamine) to warm conditions is opposite to cold conditions [61]. As opposed to sCOR that changes sensitively by stress level, BG shows a different trend by thermal state. Generally, BG increases in cold weather as the blood vessels contract. In warm weather, on the contrary, BG decreases because the blood thickens, and the blood vessels extends as moisture is discharged as sweat. Based on such scientific facts, if the occupants' bio-signal features and thermal acceptance by thermal state are considered, it is expected that a prediction model with higher predictive performance can be developed in the future.

4. Discussions

4.1. Practical implications

While related works confined their prediction models based on limited types of bio-signal features, this study suggested adding BG and COR to develop advanced thermal comfort-prediction models. This study's findings make several contributions. The results of feature importance analysis demonstrated the possibility of using BG and COR as the new bio-signal features to develop prediction models in the future. Related works have never used BG or COR as predictor variables of a prediction model by measuring them with CGMS, so this study is significant in terms of academic perspective. As shown in Fig. 8, the proposed model of which average accuracy has improved by 9.5% to the conventional model is expected to be used in the smart building systems in the near future. In the future smart buildings, occupants' BG and COR as well as many other bio-signal features can be collected in real-time from a variety of wearable devices. Wearable devices, as well as wristband, are expected to be developed in the form of smart contact lenses and needle patches. The smart contact lens placed on retina in a non-invasive way to measure hormone secretion and diabetic [62,63]. Additionally, various types of smart patches have been developed to continuously measure many bio-signals such as body temperature, heart rate etc. [64,65]. The proposed model will be able to estimate the occupants' thermal comfort using these bio-signals with high accuracy. Consequently, a suitable thermal comfort environment could be offered to occupants by operating an air conditioning system based on the predicted thermal comfort (refer to Fig. 8). Lastly, this study figured out that the importance of each bio-signal differs by gender. Suppose such gender difference is applied to the prediction model. In that case, an air conditioning system can be operated based on the gender ratio of the occupants to offer an optimal thermal comfort zone. Eventually, this will lead to enhanced work productivity and health of the occupants in the building.

4.2. Limitations and future directions

The advanced thermal comfort-prediction model proposed in this study can enhance occupants' thermal comfort in future smart buildings. However, there exist several limitations that the proposed model should overcome for its application in general conditions. First, the proposed model, at this state, has limitations in its practical application due to the unique characteristics of BG and sCOR. While the study limited the subjects' condition for an accurate measurement of BG and COR, such as forcing them not to eat for 8 h before the experiment or maintaining the condition of the mouth, etc., it is almost impossible to satisfy such conditions when the proposed model is to be applied to an actual space. In other words, BG is most affected by the occupant's diet, and COR varies greatly by the time of measurement and the condition of the mouth, so practical application of the proposed model can be limited. Second, the wearable and portable device used in this study is limited. CGMS measures the glucose in the interstitial fluid, not in blood, so there may be some difference to the glucose in the peripheral vascular system. Also, ST measured by wearable device is limited in local areas like the wrist, not in various other parts of the body, and thus, the measured values can be somewhat less versatile. Third, the exposure time was too

Fig. 8. Conceptual diagram of practical implication.

short, so it was difficult for the subjects to fully acclimatize to the experimental conditions. Likewise, the rest time was short, so the subject's bio-signals did not return to a steady state quickly. To overcome the limitations and improve the prediction model further, future research needs to pay attention to the following directions. For generalization of the proposed model, the subjects' diet and the time of data measurement should be considered. Second, it is necessary to perform experiments with diabetics whose BG level is highly varied and sensitive compared to ordinary people and subjects in various age groups with different level of functions in hormone secretion. Finally, a pilot study will be carried out before the main experiment to determine the exposure and rest time.

5. Conclusion

This study proposed an advanced thermal comfort-prediction model with 11 bio-signal features including blood glucose (BG) and salivary cortisol (sCOR) that have never been considered in previous studies. In line with the development of wearable devices such as a continuous blood glucose system, this study aimed to improve the predictive performance of conventional prediction models by adding BG and sCOR to the predictor variable. To this end, an advanced thermal comfort-prediction model based on supervised learning algorithms was proposed.

The results of this study demonstrated the following: (i) the proposed model had significantly better performance than the conventional model with 9.5% improvement in accuracy. It is noted that the feature importance of BG and sCOR was 11.8% and 10.5%, respectively, showing that they were more important than the other bio-signal features; (ii) sCOR was the most important bio-signal feature in both gender groups, and BG also was a relatively important bio-signal feature at 10.7 and 13.5%; and (iii) assessment in thermal state perspective was also carried out and it showed that BG is the most important bio-signal feature in cold condition.

The proposed model in this study implies the following contributions: (i) high importance of BG and sCOR suggested the possibility of new bio-signal features for prediction model development research in the future; (ii) it is expected that if the proposed model is applied to smart buildings, more efficient operation of the air conditioning system is possible since the proposed model estimates thermal comfort with relatively better accuracy; (iii) this study also suggested the gender difference in bio-signal and psychological measurements in various thermal environments. In other words, if gender-based importance is used, the operation of an air conditioning system can use the gender ratio of the occupants to offer an optimal thermal comfort zone.

Considering the characteristics of BG and sCOR, the variation in these predictors according to the occupants' diet or time of the measurement can be implemented to the proposed model in future research so that it could be applied to a more general condition.

CRediT authorship contribution statement

Hakpyeong Kim: Writing – original draft, Software, Resources, Methodology, Investigation, Formal analysis, Data curation. **Dahyun Jung:** Writing – original draft, Validation, Resources, Methodology, Investigation, Formal analysis, Data curation. **Heeju Choi:** Visualization, Validation, Investigation, Formal analysis, Data curation, Writing – original draft. **Taehoon Hong:** Writing – review & editing, Validation, Supervision, Project administration, Methodology, Investigation, Funding acquisition, Conceptualization.

Declaration of competing interest

The authors declare that they have no known competing financial interests or personal relationships that could have appeared to influence the work reported in this paper.

Data availability

Data will be made available on request.

Acknowledgments

This work was supported by the National Research Foundation of Korea (NRF) grant funded by the Korea government (MSIT; Ministry of Science and ICT) (NRF-2021R1A3B1076769).

Appendix

Table A1
Thermal sensation vote

Rating	−3	−2	−1	0	1	2	3
Classification	Cold	Cool	Slightly Cool	Neutral	Slightly Warm	Warm	Hot

Table A2
Thermal Preference

Rating	0	1
Classification	No preference	Preference

Table A3
STAI X-1 (Trait anxiety)

Questionnaire		Not at all	Somewhat	Moderately	Very much
1	I am always in a good mood				
2	I am tired easily				
3	I feel like crying				
4	I am happy like everyone else				
5	I can't make up mind quickly				
6	I am peaceful				
7	I am calm				
8	I can't overcome problems				
9	I am worried about trivial things				
10	I am happy				
11	I tend to think hard about anything				
12	I lack self-confidence				
13	I am at peace				
14	I try to avoid difficulties				
15	I am depressed				
16	I am satisfied				
17	I suffer from trivial things				
18	I am disappointed				
19	I am steady person				
20	I am nervous				

Table A4
STAI X-2 (State anxiety)

Questionnaire		Not at all	Somewhat	Moderately	Very much
1	I have a calm mind				
2	I am at peace				
3	I am nervous				
4	I feel regretful and sad				
5	I feel at ease				
6	I am embarrassed and do not know what to do.				
7	I am worried about future misfortune.				
8	I am at ease.				
9	I am anxious				
10	I feel comfortable				
11	I am confident				
12	I am annoyed				
13	I am nervous				
14	I am extremely nervous				
15	I am relaxed and warm				
16	I am satisfied				
17	I am warried				
18	I am so excited				
19	I am happy				
20	I feel good				

References

[1] W. Medical, D. Market, B. Application, B. Region, S. Forecasts, Report Overview (2022) 1–8. https://www.grandviewresearch.com/industry-analysis/wearable-medical-devices-market.
[2] Fitbit. https://www.fitbit.com/global/us/home.
[3] Apple, Watch (2022, July 1). https://www.apple.com/watch/.
[4] S. ichi Tanabe, M. Haneda, N. Nishihara, Workplace productivity and individual thermal satisfaction, Build. Environ. 91 (2015) 42–50, https://doi.org/10.1016/j.buildenv.2015.02.032.
[5] A. Lipczynska, S. Schiavon, L.T. Graham, Thermal comfort and self-reported productivity in an office with ceiling fans in the tropics, Build. Environ. 135 (2018) 202–212, https://doi.org/10.1016/j.buildenv.2018.03.013.
[6] A.M. Bueno, A.A. de Paula Xavier, E.E. Broday, Evaluating the connection between thermal comfort and productivity in buildings: a systematic literature review, Buildings 11 (2021), https://doi.org/10.3390/buildings11060244.
[7] Y. Wu, H. Liu, B. Li, R. Kosonen, S. Wei, J. Jokisalo, Y. Cheng, Individual thermal comfort prediction using classification tree model based on physiological parameters and thermal history in winter, Build. Simulat. 14 (2021) 1651–1665, https://doi.org/10.1007/s12273-020-0750-y.
[8] M. Burzo, C. Wicaksono, M. Abouelenien, D. Shapiro, D. Billman, M. Marker, P. Langley, T. Peffer, M. Pritoni, A. Meier, C. Aragon, D. Perry, L. Berkeley, P. Taylor, T. Peffer, D. Perry, M. Pritoni, C. Aragon, A. Meier, Multimodal sensing of thermal discomfort for adaptive energy saving in buildings, Build. Environ. 46 (2004) 2529–2541.
[9] D. Li, C.C. Menassa, V.R. Kamat, Non-intrusive interpretation of human thermal comfort through analysis of facial infrared thermography, Energy Build. 176 (2018) 246–261, https://doi.org/10.1016/j.enbuild.2018.07.025.
[10] S. Liu, M. Jin, H.P. Das, C.J. Spanos, S. Schiavon, Personal thermal comfort models based on physiological parameters measured by wearable sensors, Proc. 10th Windsor Conf.: Rethinking Comfort (2018) 431–441.
[11] J.H. Choi, D. Yeom, Development of the data-driven thermal satisfaction prediction model as a function of human physiological responses in a built environment, Build. Environ. 150 (2019) 206–218, https://doi.org/10.1016/j.buildenv.2019.01.007.
[12] Amercian diabetes associations, Clinical practice recommendations 1996, Diabetes Care 19 (1996) S1–S118. https://diabetes.org/diabetes/a1c/diagnosis.
[13] freestyle libre, Continuous Glucose Monitoring (CGM) (2022, July 1). https://www.freestylelibre.co.uk/libre/.
[14] O. Parlak, Portable and wearable real-time stress monitoring: a critical review, Sensor. Actuator. Rep. 3 (2021), https://doi.org/10.1016/j.snr.2021.100036.
[15] M. Ku, J. Kim, J.E. Won, W. Kang, Y.G. Park, J. Park, J.H. Lee, J. Cheon, H.H. Lee, J.U. Park, Smart, soft contact lens for wireless immunosensing of cortisol, Sci. Adv. 6 (2020) 1–10, https://doi.org/10.1126/sciadv.abb2891.
[16] J. Kim, M. Kong, T. Hong, K. Jeong, M. Lee, Physiological response of building occupants based on their activity and the indoor environmental quality condition changes, Build. Environ. 145 (2018) 96–103, https://doi.org/10.1016/J.BUILDENV.2018.09.018.
[17] J. Kim, H. Kim, T. Hong, Automated classification of indoor environmental quality control using stacked ensembles based on electroencephalograms, Comput. Aided Civ. Infrastruct. Eng. 35 (2020) 448–464, https://doi.org/10.1111/mice.12515.
[18] H. Kim, T. Hong, J. Kim, S. Yeom, A psychophysiological effect of indoor thermal condition on college students' learning performance through EEG measurement, Build. Environ. 184 (2020), 107223, https://doi.org/10.1016/J.BUILDENV.2020.107223.
[19] S. Jung, J. Jeoung, T. Hong, Occupant-centered real-time control of indoor temperature using deep learning algorithms, Build. Environ. 208 (2022), 108633, https://doi.org/10.1016/J.BUILDENV.2021.108633.
[20] M. Kong, H. Kim, T. Hong, An effect of numerical data through monitoring device on perception of indoor air quality, Build. Environ. 216 (2022), 109044, https://doi.org/10.1016/J.BUILDENV.2022.109044.
[21] J. Jeoung, S. Jung, T. Hong, J.K. Choi, Blockchain-based IoT system for personalized indoor temperature control, Autom. ConStruct. 140 (2022), 104339, https://doi.org/10.1016/J.AUTCON.2022.104339.
[22] S. Ngampramuan, P. Tungtong, S. Mukda, A. Jariyavilas, C. Sakulisariyaporn, Evaluation of autonomic nervous system, saliva cortisol levels, and cognitive function in major depressive disorder patients, Depress Res. Treat. (2018) 1–8, https://doi.org/10.1155/2018/7343592, 2018.
[23] J. Strahler, N. Skoluda, M.B. Kappert, U.M. Nater, Simultaneous measurement of salivary cortisol and alpha-amylase: application and recommendations, Neurosci. Biobehav. Rev. 83 (2017) 657–677, https://doi.org/10.1016/J.NEUBIOREV.2017.08.015.
[24] E.P.M. Corssmit, J.A. Romijn, H.P. Sauerwein, Review article: regulation of glucose production with special attention to nonclassical regulatory mechanisms: a review, Metabolism 50 (2001) 742–755, https://doi.org/10.1053/meta.2001.24195.
[25] S. Lindmark, U. Wiklund, P. Bjerle, J.W. Eriksson, Does the autonomic nervous system play a role in the development of insulin resistance? A study on heart rate variability in first-degree relatives of Type 2 diabetes patients and control subjects, Diabet. Med. 20 (2003) 399–405, https://doi.org/10.1046/j.1464-5491.2003.00920.x.
[26] H. Cai, A.S. McNeilly, L.M. Luttrell, B. Martin, Endocrine function in aging, Internet J. Endocrinol. (2012), https://doi.org/10.1155/2012/872478, 2012.
[27] World health organisation, 6) A Healthy Lifestyle. https://www.who.int/europe/news-room/fact-sheets/item/a-healthy-lifestyle—who-recommendations#:~:text=To%20ensure%20a%20healthy%20lifestyle,promote%20and%20support%20healthy%20lifestyles.
[28] Empatica, E4 wristband user's manual © 2018, 1, 2018, pp. 1–32.
[29] A. Rahmatillah, Y. Sa, A. Putri, Electrodermal Activity for Measuring Cognitive and Emotional Stress Level, 2022, https://doi.org/10.4103/jmss.JMSS.
[30] A.A. Romanovsky, Skin temperature: its role in thermoregulation, Acta Physiol. 210 (2014) 498–507, https://doi.org/10.1111/apha.12231.
[31] Empatica (2020, January 24) How is IBI.csv obtained? - Empatica Support. https://support.empatica.com/hc/en-us/articles/360030058011-E4-data-IBI-expected-signal.
[32] L.M. Baker, W.M. Taylor, The relationship under stress between changes in skin temperature, electrical skin resistance, and pulse rate": erratum, J. Exp. Psychol. 49 (1955) 300, https://doi.org/10.1037/h0038809.
[33] J. Wu, Z. Hu, Z. Han, Y. Gu, L. Yang, B. Sun, Human physiological responses of exposure to extremely cold environments, J. Therm. Biol. 98 (2021), 102933, https://doi.org/10.1016/j.jtherbio.2021.102933.
[34] L.J.P. van D, E.J.C. de Geus, G.M. Tanja, Vrijkotte, Effects of work stress on ambulatory blood pressure, heart rate, and heart rate variability, Hypertension 35 (4) (2000) 880–886.
[35] D. Gasperin, G. Netuveli, J.S. Dias-da-Costa, M.P. Pattussi, Effect of psychological stress on blood pressure increase: a meta-analysis of cohort studies, Cad. Saúde Pública 25 (2009) 715–726, https://doi.org/10.1590/S0102-311X2009000400002.
[36] J. Wu, Z. Hu, Z. Han, Y. Gu, L. Yang, B. Sun, Human physiological responses of exposure to extremely cold environments, J. Therm. Biol. 98 (2021), 102933, https://doi.org/10.1016/j.jtherbio.2021.102933.
[38] D.H. Hellhammer, S. Wüst, B.M. Kudielka, Salivary cortisol as a biomarker in stress research, Psychoneuroendocrinology 34 (2009) 163–171, https://doi.org/10.1016/j.psyneuen.2008.10.026.
[39] Sarstedt, Hygienic saliva collection for diagnostics and monitoring Saliva as a sample material. https://www.Sarstedt.Com/Fileadmin/User_upload/99_Broschueren/Englisch/156_Salivette_GB_0813.Pdf.
[40] ISO_7730, International standard international standard - ISO 527-1, 2012. Iso. 2012.
[41] G. Paliaga, L.J. Schoen, P.F. Alspach, E.A. Arens, R.M. Aynsley, R. Bean, J. Eddy, T. B. Hartman, D. Int-hout, M.A. Humphreys, E.E. Khalil, M.P.O. Rourke, P. Simmonds, S.C. Turner, R.L. Hall, D.T. Reindl, J.R. Anderson, C.S. Barnaby, J. A. Clark, S.J. Emmerich, P.T. Graef, Thermal environmental conditions for human occupancy, ASHRAE Standard 8400 (2010) 1–44.
[42] J. Kim, T. Hong, M. Kong, K. Jeong, Building occupants' psycho-physiological response to indoor climate and CO2 concentration changes in office buildings, Build. Environ. 169 (2020), 106596, https://doi.org/10.1016/j.buildenv.2019.106596.
[43] C.D. Spielberger, Spielberger, State-Trait Anxiety Inventory Bibliography, second ed., 1989 n.d.
[44] M. Benedek, C. Kaernbach, A continuous measure of phasic electrodermal activity, J. Neurosci. Methods 190 (2010) 80–91, https://doi.org/10.1016/j.jneumeth.2010.04.028.
[45] M. Tarvainen, L. Lipponen, R. Niskanen, P. Ranta-aho, Kubios HRV Software: User's Guide, 2016, pp. 4–40.
[46] V.R. Joseph, Optimal ratio for data splitting, Stat. Anal. Data Min. (2022) 531–538, https://doi.org/10.1002/sam.11583.
[47] K. Rewitz, D. Müller, Influence of gender, age and BMI on human physiological response and thermal sensation for transient indoor environments with displacement ventilation, Build. Environ. 219 (2022), 109045, https://doi.org/10.1016/j.buildenv.2022.109045.
[48] M. Indraganti, M.A. Humphreys, A comparative study of gender differences in thermal comfort and environmental satisfaction in air-conditioned offices in Qatar, India, and Japan, Build. Environ. 206 (2021), 108297, https://doi.org/10.1016/j.buildenv.2021.108297.
[49] T. Chaudhuri, D. Zhai, Y.C. Soh, H. Li, L. Xie, Random forest based thermal comfort prediction from gender-specific physiological parameters using wearable sensing technology, Energy Build. 166 (2018) 391–406, https://doi.org/10.1016/j.enbuild.2018.02.035.
[50] H. Liu, Y. Wu, D. Lei, B. Li, Gender differences in physiological and psychological responses to the thermal environment with varying clothing ensembles, Build. Environ. 141 (2018) 45–54, https://doi.org/10.1016/j.buildenv.2018.05.040.
[51] J. Xiong, Z. Lian, X. Zhou, J. You, Y. Lin, Investigation of gender difference in human response to temperature step changes, Physiol. Behav. 151 (2015) 426–440, https://doi.org/10.1016/j.physbeh.2015.07.037.
[52] M. Indraganti, M.A. Humphreys, A comparative study of gender differences in thermal comfort and environmental satisfaction in air-conditioned offices in Qatar, India, and Japan, Build. Environ. 206 (2021), 108297, https://doi.org/10.1016/j.buildenv.2021.108297.
[53] H. Liu, Y. Wu, D. Lei, B. Li, Gender differences in physiological and psychological responses to the thermal environment with varying clothing ensembles, Build. Environ. 141 (2018) 45–54, https://doi.org/10.1016/j.buildenv.2018.05.040.
[54] J. Xiong, Z. Lian, X. Zhou, J. You, Y. Lin, Investigation of gender difference in human response to temperature step changes, Physiol. Behav. 151 (2015) 426–440, https://doi.org/10.1016/j.physbeh.2015.07.037.
[55] J.H. Choi, D. Yeom, Development of the data-driven thermal satisfaction prediction model as a function of human physiological responses in a built environment, Build. Environ. 150 (2019) 206–218, https://doi.org/10.1016/j.buildenv.2019.01.007.
[56] T. Chaudhuri, Y.C. Soh, H. Li, L. Xie, Machine learning driven personal comfort prediction by wearable sensing of pulse rate and skin temperature, Build. Environ. 170 (2020), 106615, https://doi.org/10.1016/j.buildenv.2019.106615.

[57] R.A. Sicree, P.Z. Zimmet, D.W. Dunstan, A.J. Cameron, T.A. Welborn, J.E. Shaw, Differences in height explain gender differences in the response to the oral glucose tolerance test - the AusDiab study, Diabet. Med. 25 (2008) 296–302, https://doi.org/10.1111/j.1464-5491.2007.02362.x.
[58] F. Mauvais-Jarvis, Gender differences in glucose homeostasis and diabetes, Physiol. Behav. 187 (2018) 20–23, https://doi.org/10.1016/j.physbeh.2017.08.016.
[59] C. Otte, S. Hart, T.C. Neylan, C.R. Marmar, K. Yaffe, D.C. Mohr, A meta-analysis of cortisol response to challenge in human aging: importance of gender, Psychoneuroendocrinology 30 (2005) 80–91, https://doi.org/10.1016/j.psyneuen.2004.06.002.
[60] J. Xiong, Z. Lian, H. Zhang, Effects of exposure to winter temperature step-changes on human subjective perceptions, Build. Environ. 107 (2016) 226–234, https://doi.org/10.1016/j.buildenv.2016.08.002.
[61] S. Hu, M. He, X. Zhang, H. Guan, P. Song, R. Liu, G. Liu, Cold and hot step-changes affecting thermal comfort and physiological indicators in winter, Energy Build. 254 (2022), 111587, https://doi.org/10.1016/j.enbuild.2021.111587.
[62] J. Park, J. Kim, S.-Y. Kim, W.H. Cheong, J. Jang, Y.-G. Park, K. Na, Y.-T. Kim, J. H. Heo, C.Y. Lee, J.H. Lee, F. Bien, J.-U. Park, Soft, smart contact lenses with integrations of wireless circuits, glucose sensors, and displays, Sci. Adv. 4 (2018), https://doi.org/10.1126/sciadv.aap9841.
[63] D.H. Keum, S.-K. Kim, J. Koo, G.-H. Lee, C. Jeon, J.W. Mok, B.H. Mun, K.J. Lee, E. Kamrani, C.-K. Joo, S. Shin, J.-Y. Sim, D. Myung, S.H. Yun, Z. Bao, S.K. Hahn, Wireless smart contact lens for diabetic diagnosis and therapy, Sci. Adv. 6 (2020), https://doi.org/10.1126/sciadv.aba3252.
[64] M.A. Invernale, B.C. Tang, R.L. York, L. Le, D.Y. Hou, D.G. Anderson, Microneedle electrodes toward an amperometric glucose-sensing smart patch, Adv. Healthc. Mater. 3 (2014) 338–342, https://doi.org/10.1002/adhm.201300142.
[65] H. Kim, S. Kim, M. Lee, Y. Rhee, S. Lee, Y.-R. Jeong, S. Kang, M. Naqi, S. Hong, Smart patch for skin temperature: preliminary study to evaluate psychometrics and feasibility, Sensors 21 (2021) 1855, https://doi.org/10.3390/s21051855.